

# DESIGN OF A RETRACTABLE LANDING GEAR FOR THE SAGITTA DEMONSTRATOR UAV

Florian Nikodem, Frank Möller, Patrick Gallun, Andreas Bierig,  
Institute of Flight System, German Aerospace Center (DLR)  
38108 Braunschweig, Germany

## Abstract

This paper gives an overview about the development of the retractable landing gear for the SAGITTA demonstrator, a flight testbed for future UCAV (Unmanned Combat Air Vehicle). Due to the special requirements of the SAGITTA Demonstrator and the lack of suitable COTS (Commercial-of-the-Shelf) solutions available on the market, an entirely new development of the retractable landing gear was necessary. The first part of this paper describes the design process and the special challenges for the development of a small high-performance landing gear under the technical constraints of the SAGITTA project. Subsequently, the landing gear development including shock absorber and brake system design and the tests, carried out at the specially developed test stand, are discussed. The main focus lies on the use of handbook formulae for larger aircrafts landing gear design that are applied to the requirements of a small UAV in this paper. The conducted drop-tests of the developed landing gear showed satisfying results.

## NOMENCLATURE

$a_{brk}$	Deceleration while braking	$n_s$	Efficiency factor of the shock absorber
$a_{ideal}$	Ideal constant acceleration	$n_t$	Efficiency factor of the tire
$A_{pad}$	Surface area of the brake pad	$p_{brake}$	Pressure in the brake lane
$A_{cyl}$	Surface area of the brake cylinder	$R$	Spring rate
$c$	Damper characteristic	$S$	Stroke of the shock absorber
$c$	Specific heat capacity	$S_{min}$	Minimum brake disk thickness
$c_{xd}$	Damper characteristic depending on the used stroke	$S_t$	Tire deflection under maximum load factor
$d_{disc}$	Diameter of the brake disk	$t$	Time
$d_{wheel}$	Diameter of the main landing gear wheel	$T_{ambient}$	Ambient temperature
$E_{kin}$	Kinetic energy	$T_{max}$	Maximum allowed temperature
$F_{act}$	Force delivered by the actuator	$V$	Vertical landing speed
$F_{brake}$	Brake force	$V_{AC}$	Velocity of the aircraft
$F_{brake,act,max}$	Maximum brake force of the actuator	$V_{xd}$	Damper compressing speed depending on the used stroke
$F_{brake,max}$	Maximum allowed brake force without wheel block	$X_d$	Used stroke of the damper
$F_{M max}$	Maximum static load of one main landing gear leg	$X_t static$	Used stroke in static position
$F_N$	Normal force	$\Delta Q$	Transferred amount of heat
$F_{N max}$	Maximum static load on the nose gear	$\Delta T$	Temperature difference
$F_{N max, brk}$	Maximum load on the nose gear while braking	$\mu_{pad}$	Friction coefficient of brake pad and brake disk
$F_{pad}$	Force at the brake pad	$\mu_t$	Friction coefficient of tire and runway
$g$	Gravity acceleration	$\rho$	Density of the disk brake material
$i$	Transmission coefficient of the brake system	CoG	Center of Gravity
$K$	Lift to weight ratio of the aircraft	COTS	Commercial-of-the-Shelf
$m_{AC}$	Mass of the aircraft	EMA	Electromechanical Actuator
$M_{caliper}$	Torque at the caliper	FCC	Flight Control Computer
$m_{disc}$	Mass of the brake disk	LO	Low Observability
$m_{TOW}$	Maximum take-off weight of the aircraft	MEA	More Electric Aircraft
$M_{wheel}$	Torque at the wheel	MLG	Main Landing Gear
$N$	Reaction load factor; the static load plus the dynamic reaction load at touch-down divided by the static load	MLG RH	Main Landing Gear right hand side
		MMC	Mission Management Computer
		MTOW	Maximum Take-Off Weight
		NLG	Nose Landing Gear
		PWM	Pulse Width Modulation
		UAV	Unmanned Air Vehicle
		UCAV	Unmanned Combat Air Vehicle

## 1. THE SAGITTA DEMONSTRATOR UAV

SAGITTA is a project conducted in the framework of Open Innovation, whereby industry and research institutes foster a cooperation with the aim of combining technical and business competencies as well as innovative technologies of all partners to achieve accelerated technical progress. SAGITTA was initiated in 2011 by Airbus Defense and Space together with numerous institutes of German universities and the German Aerospace Center (DLR). The project finished successfully with the maiden flight of the demonstrator in July 2017.

The purpose of the project was to carry out research on promising technology for futureUCAV and to demonstrate those technologies on a flying testbed. Hence, the realization of the flying testbed became one of the major goals. The research areas addressed by the project are aerodynamics, flight control and guidance, autonomous mission management, overall aircraft design, design and manufacturing technologies for lightweight structures and system design towards the More Electric Aircraft (MEA) [1].

The SAGITTA Demonstrator UAV (Unmanned Air Vehicle) is a 1 to 4 downscaled version of a reference aircraft of Airbus Defense and Space [2]. As shown in FIGURE 1, the aircraft exhibits a diamond shaped design without a vertical tail in order to minimize the radar cross section and hence yield a Low Observability optimized design. It has a wing span and a length of app. 3 m and is propelled by two jet engines, each developing a maximum thrust of 250 N. As innovative approach in LO technology, all openings, such as air intakes and outlets as well as maintenance and landing gear doors, are located at the lower skin of the aircraft. The upper, so called "clean", skin of the aircraft is free of any gap and hence optimized to reflect as less radar signals as possible. The aircraft has the capability to fly in inverted position, whereby the clean skin points to the ground, respectively to the radar stations.

To demonstrate new design and manufacturing approaches, the entire structure of the aircraft is made from carbon fiber. The flight control surfaces are two in-board flaps for pitch control, two mid-board flaps for roll control and four out-board split flaps, two at each wing tip, to produce yawing moments. Each of the eight control surfaces is driven by an electromechanical actuator.

To realize autonomy functions, a complex avionics system is installed into the aircraft. The main computers are the FCC and the MMC. The FCC realizes all low level flight control functions, such as stability augmentation and waypoint navigation. The MMC contains complex high level functions, e.g. decision management for autonomous mission re-planning [3].

The systems and functions of the SAGITTA Demonstrator are either categorized as flight-critical or non-flight-critical. The design team chose a well-tested simplex system instead of a system with redundancies. Therefore the risk of single points of failures of flight-critical systems that may lead to the loss of aircraft has to be considered. The development effort of such simplex systems is also significantly less in comparison with a fully fault tolerant design.

Since the landing gear of the aircraft is classified as flight-critical a robust design as well as an intense test program was demanded to proof its suitability for the aircraft. Therefore, this paper deals with the design and development of the landing gear in the framework of the

SAGITTA project. In this paper, section 2 gives an overview about the SAGITTA Demonstrator landing gear. Section 3 provides a detailed explanation of the landing gear design including the shock absorber design, the brake system design as well as the tire selection. In section 4 the landing gear testbed and the landing gear qualification tests are described.

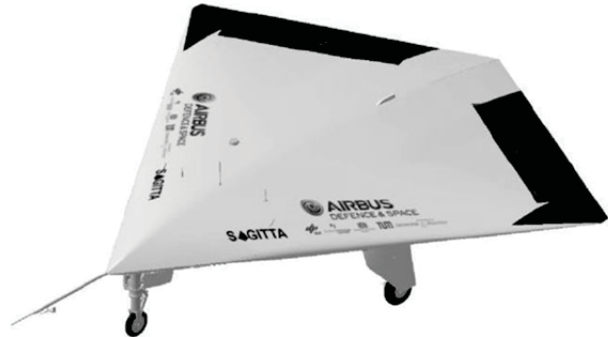


FIGURE 1. SAGITTA Demonstrator UAV

## 2. OVERVIEW ABOUT THE SAGITTA LANDING GEAR

The design of the landing gear for the SAGITTA Demonstrator was a comprehensive task. To enable the capability for continuous inverted flight, it was clear from the very beginning of the project that an entirely retractable landing gear is necessary. Further, it was considered, that a safety pilot must be able to land the aircraft manually by means of a remote control, which may lead to significantly high vertical speeds during touch down. Hence, the design team derived a set of requirements for the SAGITTA Demonstrator. The major design requirements of the landing gear were:

- Maximum vertical approach speed of 2.5 m/s
- Maximum horizontal approach speed of 49 m/s
- Maximum start abort speed of 41 m/s
- Maximum take-off weight (MTOW) of 150 kg
- Maximum landing weight of 125 kg
- Maximum drop down force of 5 kN
- The landing gear has to be retractable
- The space in the fuselage is very limited

Since there was no commercial landing gear available that fulfilled these requirements, the development of a new landing gear from the scratch was necessary. Despite not being an actual research topic of the Open Innovation Project it became clear that landing gear design is a quite comprehensive task.

The chosen design of the landing gear exhibits a tricycle layout. Each landing gear has one wheel and spring/oil-damper assembly to reduce the loads during landing. The necessary stroke is realized by a telescopic slide, which is considered as the most compact and lightweight architecture for the landing gear leg. Each landing gear leg is mostly made of anodized aluminum for weight saving reasons. Only the lower sliding tube is made of nitrided steel for increased sliding performance under high loads.

The right hand side main landing gear is shown in FIGURE 2. In addition to the wheels and the damper, the main landing gear is also equipped with a braking system. The braking system uses a hydraulic brake fluid while the

actual brake lever is operated by an electromechanical actuator. The side strut is foldable to achieve landing gear retraction. To guarantee a stable extension, the landing gear will be locked by over centered position of the side struts. In retracted position the linkage is designed to be in a dead center. The extension and retraction are also done by an EMA. The total weight of one MLG leg amounts to 4.0 kg.

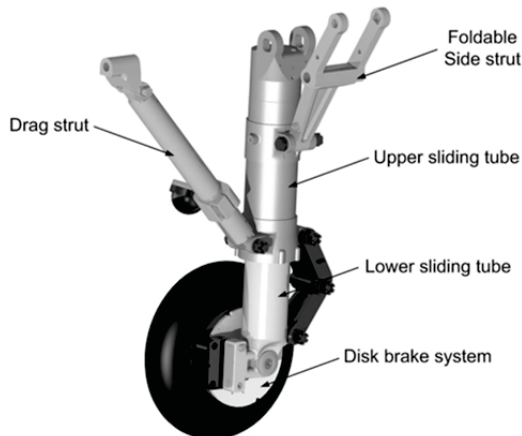


FIGURE 2. SAGITTA Demonstrator MLG RH

The design of the nose landing gear is shown in FIGURE 3. The nose wheel provides also the steering function for the aircraft on ground. For this purpose an electromechanical actuator, which is attached by a tooth belt assembly, deflects the nose-wheel.

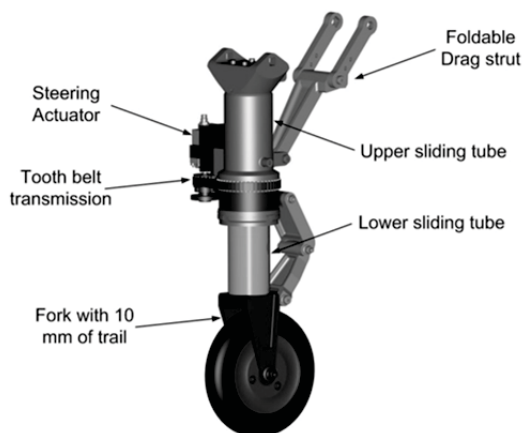


FIGURE 3. SAGITTA Demonstrator NLG

The Nose Landing Gear (NLG) shown in FIGURE 3 is steerable by an attached EMA and a tooth belt transmission. The NLG is able to rotate approximately 23° to the right side in flight direction and 90° to the left to allow full retraction. The overall retraction/extension mechanism with locked and over centered position is basically the same as the mechanism at the MLG. The total weight of the NLG amounts to 3.5 kg.

### 3. DETAILED DESIGN CONSIDERATIONS FOR THE LANDING GEAR

This section describes the development process of the SAGITTA Demonstrator UAV landing gear. This comprises the shock absorber and brake system design

as well as tire selection. The design process of the landing gear followed a classical systems engineering approach [4]. After clarifying the technical requirements and functions, different candidate solutions have been evaluated during a pre-design phase. The most suitable concept was then selected and further developed in the subsequently followed detailed design phase. Already in this phase many engineering tests have been conducted to deeply investigate design principles. After solving all design issues and completion of the design, the final landing gear for flight purpose was built and verified on a special testbed. Most of the validation activities have been conducted after installation into the aircraft and performing taxi- as well as first flight tests.

The landing gear attachment points were defined in the preliminary design phase of the demonstrator. The landing gear design is restricted by these pre-design decisions. The defined wheelbase of the demonstrator is shown in FIGURE 4, while FIGURE 5 gives a more detailed view of the landing gear geometry and the center of gravity (CoG) limitations.

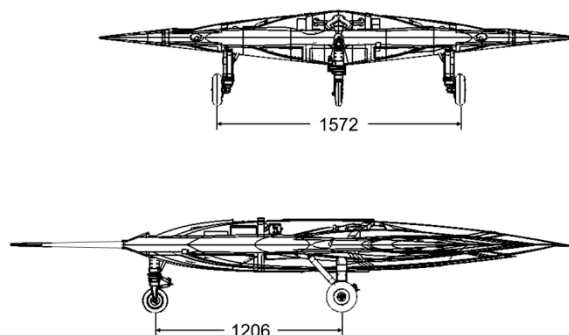


FIGURE 4. SAGITTA Demonstrator wheelbase

FIGURE 5 shows the position and height of the most forward and the most aft CoG relative to the NLG. All measures were determined in the preliminary design phase. Due to the design of the demonstrator the CoG in static position, that means the aircraft is on ground with MTOW, is located 143 mm in front of the MLG leading to a weight distribution of around 85% on the MLG and 15% on the NLG. The CoG in static position being the CoG in most aft position is rather special, since most aircrafts have their CoG in static position somewhere between most forward and most aft position.

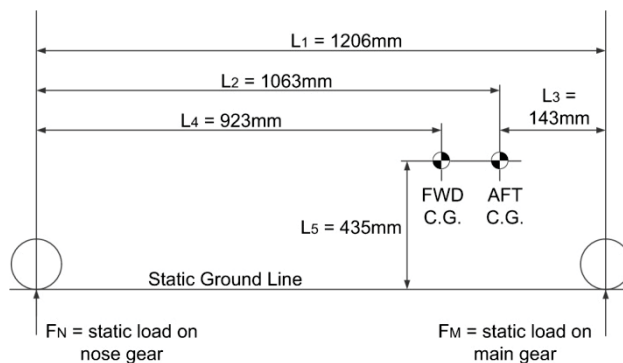


FIGURE 5. SAGITTA Demonstrator geometry

### 3.1. Shock Absorber Design

The chosen simple approach is the development of the shock absorber with basic formulae found in literature. The formulae are normally used to preliminary design larger aircraft landing gears. The scientific question to be answered is whether the formulae are appropriate for the requirements of small UAV like SAGITTA demonstrator as well and offer satisfying results. In this paper the design of the MLG shock absorber is shown. The single steps of the NLG shock absorber design are similar, even though the damper characteristic will be different due to different loads on the NLG [5].

Before the damping characteristic can be set up, the shock absorbers stroke has to be determined. According to Currey the stroke depends on the landing speeds and load factors at the moment of landing. To estimate the needed stroke  $S$  at a given speed, following equation is used [5]:

$$(1) \quad S = \frac{\frac{V^2}{2 \cdot g} + S_t \cdot K \cdot S_t \cdot N \cdot S_t \cdot n_t}{N \cdot n_s - 1 + K}$$

$V$  is the vertical landing speed of 2.5 m/s,  $g$  the gravity acceleration,  $K$  is the lift to weight ratio of the aircraft,  $N$  the reaction load factor,  $S_t$  the tire deflection under maximum load factor,  $n_t$  is an efficiency factor of the tire used and  $n_s$  an efficiency factor of the shock absorber. It is recommended by Currey to set  $n_t$  to 0.47 and  $n_s$  to 0.8 for an oleo-pneumatic shock absorber. Based on the recommendations of Currey and the strict design requirements of the demonstrator (high vertical landing speed and the weight) the reaction load factor is set to 5, while the lift to weight ratio is 0.67 [6]. Since the tire diameter is 200 mm and the rim diameter is 88.9 mm, it is estimated that the tire deflection under maximum load will be around more than half of the tire sidewall height. Therefore the tire deflection is set to 35 mm. The stroke  $S$  calculated with equation (1) is 67.5 mm. Currey recommends adding 25.4 mm to the calculated stroke as safety margin. However, due to very limited space inside the SAGITTA demonstrator landing gear bays it is only possible to raise the total stroke to 70 mm. Therefore in this project a safety margin of 2.5 mm is added to the calculated stroke. A similar equation to (1) with the same recommendations is given in [7] by J. Roskam.

After the stroke is set, the characteristic of the damper can be determined. In case of the SAGITTA Demonstrator the goal was to reduce the vertical landing speed to zero with minimum peak acceleration. To do so the acceleration has to be constant over the whole stroke. That ideal constant acceleration  $a_{ideal}$  can be calculated with:

$$(2) \quad S = \frac{1}{2} \cdot a_{ideal} \cdot t^2$$

$$(3) \quad V = a_{ideal} \cdot t$$

From (2) and (3) combined follows:

$$(4) \quad a_{ideal} = \frac{V^2}{2 \cdot S}$$

To determine the damper characteristic  $c$ , depending on the dampers stroke, it can be written:

$$(5) \quad c = \frac{m_{AC} \cdot a_{ideal}}{V(x_d)}$$

The speed as a function of the stroke can be obtained from:

$$(6) \quad x_d = S - \left( \frac{V_{x_d}^2}{2 \cdot a_{ideal}} \right)$$

$$(7) \quad V_{x_d} = \sqrt{2 \cdot a_{ideal} \cdot (S - x_d)}$$

Now for the damper coefficient follows:

$$(8) \quad c_{x_d} = \frac{1.2 \cdot m_{AC} \cdot \sqrt{a_{ideal}}}{\sqrt{2 \cdot (S - x_d)}}$$

A safety factor of 1.2 for the damper characteristic is considered to take uncertainties into account such as flexibility of the whole strut and nonlinear properties of tire and damper. The inclusion of the safety factor is advantageous as well as disadvantageous. The safety factor reduces the risk of bottoming out the damper, on the contrary the higher the safety factor is chosen the higher are the landing loads on the structure of the UAV. However, drop-tests on the landing gear testbed have proven that a factor of 1.2 was a good choice for the SAGITTA Demonstrator. The resulting damper characteristic curve is shown in FIGURE 6.

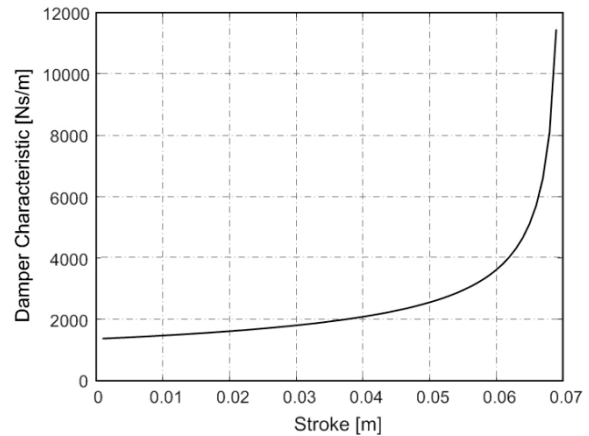


FIGURE 6. Damper characteristic curve of the MLG

The final shock absorber assembly is shown in FIGURE 7. The assembly consists of mounting points in the stub axle and the shock absorber dome, the hydraulic industrial shock absorber with the calculated stroke and the applied damper characteristic, as well as a coil spring. In difference to the normal use and characteristic of an industrial shock absorber, the damper characteristic is adjusted to the needs of a landing gear shock absorber. A common industrial shock absorber is designed to absorb most kinetic energy in the middle of its stroke, while the absorption at the begin and the end of the stroke is close to zero. To overcome its breakaway torque the landing gear shock absorber needs to have precise energy absorption at the beginning of the stroke, nearly constant energy absorption in the middle of the stroke and fast increasing energy absorption at the end of the stroke. Zimmer Group possesses the technology to adapt one of their industrial shock absorbers to a characteristic shown in FIGURE 6 [8].

The coil spring is designed to maintain the static position of the aircraft and to turn the impacts from the runway into



mechanical vibrations. These mechanical vibrations are compensated by the damper. A recommendation of [5] for a suitable floor height, the height of the aircraft in static position, is a ratio of 4/1 from static to extend. Although this is a recommendation for larger aircraft like cargo aircraft, the demonstrator is considered quite heavy for its size. Therefore a ratio of 4/1 seems to be a decent approach. Taking that into account, the static position of the aircraft is around 52.5 mm of stroke from fully extended position. The spring rate has to be designed to apply a spring force equal to the maximum static load of one landing gear leg. The spring rate  $R$  can be calculated with:

$$(9) \quad R = \frac{F_{M \max}}{x_{t \text{ static}}}$$

The maximum static load of one MLG leg  $F_{M \max}$  is calculated in TAB. 1 and  $x_{t \text{ static}}$  is the used stroke in static position. The calculated spring rate is  $R = 12.4 \text{ N/mm}$  for the MLG and  $R = 3.3 \text{ N/mm}$  for the NLG.

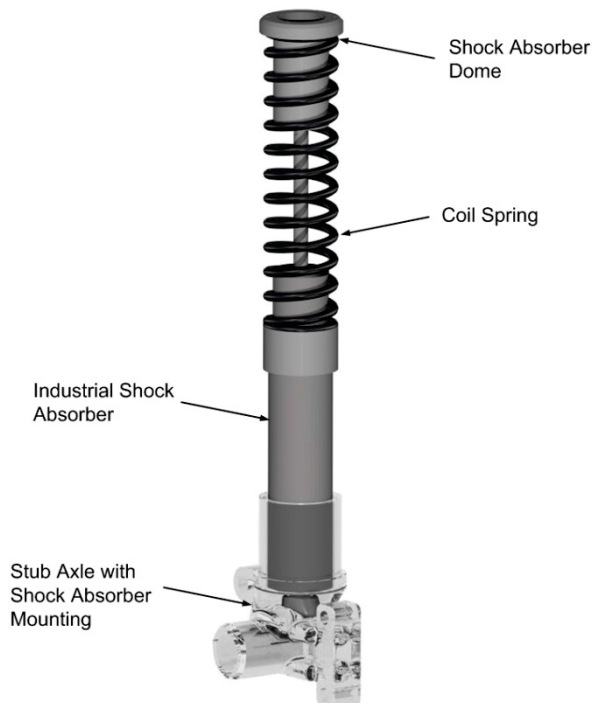


FIGURE 7. Shock absorber assembly of the main landing gear

### 3.2. Brake System Design

The SAGITTA Demonstrator is equipped with a disk brake system attached to each main landing gear leg. An EMA of the DA-26 class by Volz Servos [9] is preferred as brake actuator while the goal was to use as few different types of actuators as possible. The EMA of the DA-26 class were also supposed to be used to extend and retract the landing gear and are able to generate 5 Nm peak torque. The principle of the brake system can be seen in FIGURE 8. The actuator receives a command signal with pulse-width modulation (PWM) between 1000  $\mu\text{s}$  and 2000  $\mu\text{s}$ . Each pulse-width of the PWM signal is allocated certain torque. The actuator pushes the brake cylinder via a lever further down into the expansion tank. Both caliper of each main landing gear leg are attached to the same expansion tank,

comparable to the front brake of a motorcycle.

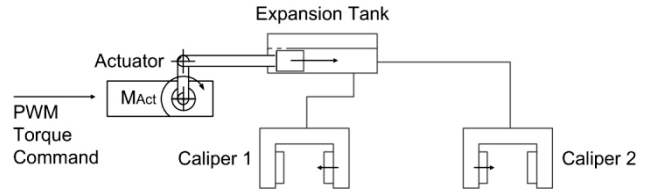


FIGURE 8. Brake system schematic

To size the brake system of an aircraft there are two major design cases which can be used. One is the braking process after rejected takeoff. The second case is the braking at maximum landing speed. Regarding the kinetic energy that has to be dissipated through deceleration, the dominant design case can be calculated.

$$(10) \quad E_{kin} = \frac{m_{AC}}{2} \cdot V_{AC}^2$$

In case of rejected takeoff the kinetic energy is 126 kJ whereas in case of braking after landing 150 kJ of kinetic energy have to be dissipated. In conclusion the braking after landing is the dominant design case.

Now the thickness of the brake disc that has to dissipate the kinetic energy into heat energy can be calculated as follows. Using the equation for specific heat capacity  $c$ :

$$(11) \quad c = \frac{\Delta Q}{m_{disc} \cdot \Delta T}$$

with

$$(12) \quad \Delta Q = \frac{m_{AC}}{4} \cdot V_{AC}^2$$

and

$$(13) \quad m_{disc} = \pi \cdot \frac{d_{disc}^2}{4} \cdot \rho \cdot s_{min}$$

the equation for the minimum disc thickness can be achieved:

$$(14) \quad s_{min} = \frac{m_{AC} \cdot V_{AC}^2}{\pi \cdot d_{disc}^2 \cdot \rho \cdot c \cdot (T_{max} - T_{ambient})}$$

with the diameter of the disc  $d_{disc}$ , that is limited by the diameter of the rim and therefore set to 120 mm, the density of the disc brake material  $\rho$ ,  $T_{max}$  the maximum allowed temperature and  $T_{ambient}$  the ambient temperature, assumed to be 20° C. For the density of the disc brake the density of steel was used. The maximum temperature of the disc was defined by the manufacturer and set to 500° C. The minimum disc thickness can be calculated to 4.5 mm. Because of space limitations the disc thickness has to be reduced to 4 mm. Since the disc is dissipating heat to the floating ambient air, it can be assumed that the disc will not reach its maximum temperature even with slightly reduced thickness. To prove this assumption the brake disk was tested on a testbed, decelerating several times, without floating air, from 49 m/s to zero and never failed once.

Now the maximum required brake force can be calculated to determine if the DA-26 actuator can also be used as brake actuator. The maximum possible brake force depends on the friction coefficient of runway and tire  $\mu_t$  as well as on the normal force  $F_N$ . Exceeding the normal

force results in wheel block, which has to be avoided to not lose control of the aircraft. Since the dynamic weight distribution will move the CoG towards the front of the aircraft, the CoG in forward position (FIGURE 5) will be considered for this calculation. Using the equilibrium of momentum in FIGURE 5, the normal force  $F_N$  depending on  $F_{brake}$  can be determined by:

$$(15) \quad F_N = \frac{m_{AC} \cdot g \cdot L_4 - F_{brake} \cdot L_5}{L_1}$$

Now  $F_N$  is substituted by the maximum allowed brake force multiplied by the friction coefficient of runway and tire  $\mu_t \cdot F_{brake, max}$ . Additionally a safety factor of 1.5 is taken into account.

$$(16) \quad F_{brake, max} = \frac{\mu_t \cdot m_{AC} \cdot g \cdot L_4}{1.5 \cdot (L_1 + \mu_t \cdot L_5)}$$

Estimating a friction coefficient  $\mu_t$  of 0.8 equation (16) leads to a maximum allowed brake force  $F_{brake, max}$  of 388 N. The maximum deceleration  $a_{brk}$  can now be calculated to

$$(17) \quad a_{brk} = \frac{F_{brake, max}}{m_{AC}}$$

To determine the maximum actuator brake force the friction coefficient of the brake pad  $\mu_{pad}$ , as well as the transmission ratio from the brake cylinder to the caliper and from disk to wheel, have to be considered. Since there are two calipers operated by one actuator the brake force distribution to each wheel has to be taken into account. It is assumed that the brake force distribution is equal on each wheel. The maximum actuator brake force can be calculated with:

$$(18) \quad F_{brake, act, max} = i \cdot \mu_{pad} \cdot \frac{F_{brake, max}}{2}$$

The transmission coefficient  $i$  contains the above mentioned transmission ratios and can be determined by following equations:

$$(19) \quad p_{brake} = \frac{F_{act}}{A_{cyl}}$$

with  $p_{brake}$  being the pressure in the brake lane,  $F_{act}$  the force delivered by the actuator and  $A_{cyl}$  the surface area of the brake cylinder. The force at the brake pad can be calculated by:

$$(20) \quad F_{pad} = p_{brake} \cdot A_{pad}$$

with  $A_{pad}$  as the surface area of the brake pad. From (19) and (20) follows:

$$(21) \quad F_{pad} = \frac{A_{pad}}{A_{cyl}} \cdot F_{act}$$

Now the transmission ratio from caliper to wheel can be taken into account:

$$(22) \quad M_{caliper} = \frac{d_{disc}}{2} \cdot F_{pad}$$

$$(23) \quad M_{wheel} = \frac{d_{wheel}}{2} \cdot F_{pad}$$

with  $d_{disc}$  being the brake disc diameter of 120 mm and  $d_{wheel}$  being the wheel diameter of 200 mm, the transmission coefficient can now be calculated by:

$$(24) \quad i = \frac{M_{wheel}}{M_{caliper}} = \frac{d_{wheel}}{d_{disc}}$$

According to equation (18), with a brake pad friction coefficient of 0.4, the maximum required brake force of the actuator can be calculated to 132 N. With a peak torque of 5 Nm and a lever arm of 20 mm resulting in possible 250 N the DA-26 actuator is well suited as brake actuator.

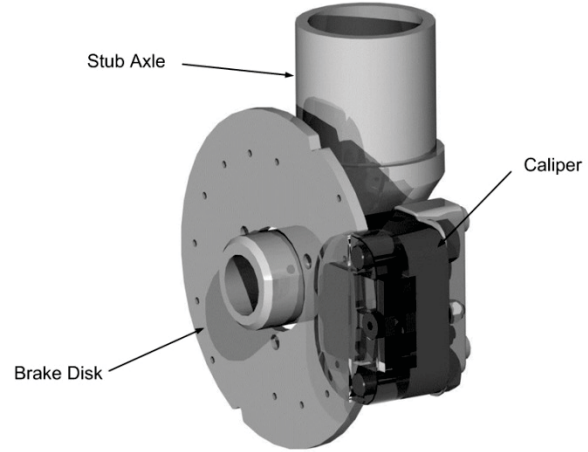


FIGURE 9. Disk brake assembly

The figure above shows the disk brake assembly of one landing gear leg of the SAGITTA Demonstrator. The disc is attached to the not displayed rim. The caliper has a floating position with one moving piston in it.

### 3.3. Tire Selection

The tire selection for a UAV of the scale of the SAGITTA Demonstrator and the requirements mentioned in section 2 is not an easy task. The main design parameters for the tire selection are the static load and the maximum peak load on each tire, as well as the maximum attained speed on ground [1]. As mentioned above the shock absorber is designed to limit the maximum landing load to 5 kN. It is assumed that in the moment of touch down the load is not distributed equally to both main gear legs. Therefore the maximum peak load per main gear tire is assumed to be 4 kN. Using the balance of moments in FIGURE 5 the maximum static load on each main gear is:

$$(25) \quad F_{M max} = \frac{m_{TOW} \cdot g \cdot L_2}{2 \cdot L_1}$$

The maximum static load on the nose gear can be calculated to:

$$(26) \quad F_{N max} = \frac{m_{TOW} \cdot g \cdot L_3}{L_1}$$

The crucial design parameter for the nose wheel is the maximum nose gear load for a given deceleration  $a_{brk}$ . With the value of  $a_{brk} = 3.1 \text{ m/s}^2$ , calculated in section 3.2, the maximum nose gear load can be determined by:

$$(27) \quad F_{N max, brk} = \frac{m_{TOW} \cdot g \cdot (L_1 - L_4)}{L_1} + \frac{m_{TOW} \cdot a_{brk} \cdot L_5}{L_1}$$

The calculated values can be seen in TAB. 1.

Force	Value [N]
$F_{M\ max}$	648.5
$F_{N\ max}$	174.5
$F_{N\ max,brk}$	513.0

TAB. 1 Calculated tire loads

The only available tires that complied with the required loads were the Aero Max II 3.5 inch and the Aero Mini 150 tires with rims by TOST. These tires are originally sailplane tires with aircraft approval. The maximum allowed static load is 2.5 kN and the maximum allowed peak load is 4 kN. Since these tires are meant for sailplane use the maximum allowed and tested speed by manufacturer is 36 m/s they are also qualified on the landing gear testbed.

#### 4. LANDING GEAR QUALIFICATION TESTING

Up to this point the landing gear design was based on standard formulae with different simplifications and assumptions. To prove these and the whole landing gear design, several test campaigns have to be carried out on a specially developed testbed. Components that need to be tested are the shock absorber, the brake system and the tires. As seen in FIGURE 10 the testbed design is strongly influenced by traditional landing gear testbeds with a rotating drum.

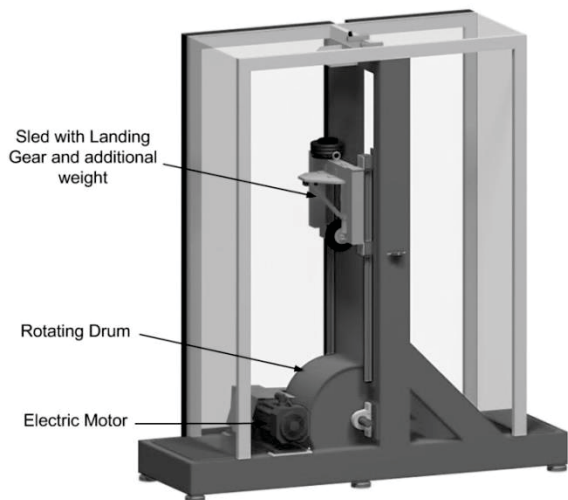


FIGURE 10. Landing gear testbed

The electric motor has a power output of 15.1 kW and 50.5 Nm of torque. The motor drives the drum via tooth belt transmission and is able to accelerate the drum up to a rotational speed equivalent to a velocity of the landing aircraft of 50 m/s. The landing gear leg is mounted in a sled that can be pulled up to a height that equals a vertical landing speed of 2.8 m/s. To be able to test MLG and NLG with the same testbed the sled can be equipped with additional weight to meet the actual weight distribution between NLG and each MLG leg. On the running surfaces of the landing gear legs the drum is not painted. The friction coefficient of raw steel and a tire is around 0.5 and equals the friction coefficient of wet asphalt and tire.

The loads at drop down on the drum are measured by three piezo electric force sensors integrated in the landing

gear mounting. The total resulting load can be obtained by superposition of the force data of all three sensors. The linear guidance of the sled is equipped with a magnetostrictive linear position sensor. The sensor measures the height of the sled to get a feedback of the horizontal speed. It is also used to measure the suspension performance after drop down. The usual test procedure contains landing gear drops at different drum speeds of 0 m/s, 30 m/s, 43.5 m/s and 49 m/s plus different vertical speeds of 1 m/s, 2 m/s and 2.5 m/s. That makes a total of 12 test cases in each test procedure.

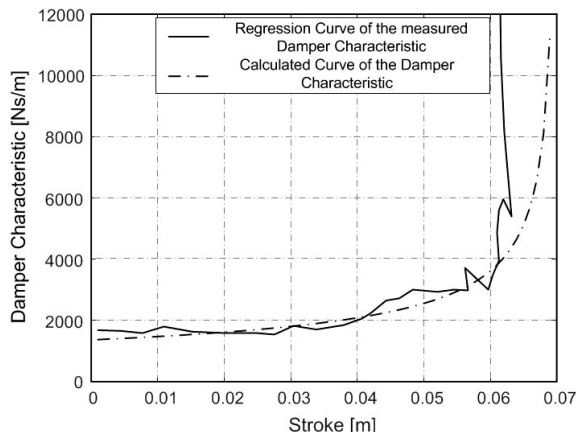


FIGURE 11. Comparison of the calculated and the measured damper characteristic

The testbed measures drop down force, stroke and vertical speed of the moment of drop down. With these measurements an actual damper characteristic (FIGURE 11) can be determined with equation (5). FIGURE 11 also shows a comparison of the calculated design damper characteristic curve (dashed line) and the measured damper characteristic curve (straight line). The shown curve resembles the actual measured raw data. It has to be kept in mind that the test data is also influenced by the damping of the tire and the flexibility of the whole strut. However in the beginning of the stroke and especially in the mid, the real damper characteristic matches the calculated ideal one quite well. It must be kept in mind that FIGURE 11 only shows the final damper characteristic in comparison. In practice several industrial damper with different predefined characteristics and different oil were tested to achieve a characteristic as close as possible to the required one.

Some of the test results of the right main landing gear are shown in TAB. 2. It can be seen that the maximum drop down force does not exceed 4.5 kN under landing conditions of 2.5 m/s vertical and 49 m/s horizontal velocity.

maximum Force [N]	$V_{vertical}$ [m/s]	$V_{horizontal}$ [m/s]
4500	2.5	0.0
4250	2.5	30.0
4500	2.5	41.3
4500	2.5	49.0
2500	1.5	41.3
3250	2.0	41.3
4500	2.5	41.3

TAB. 2 Maximum drop down force of the right MLG

A special challenge which occurred during the drop-tests was the material of the landing gear. The engineering version of the landing gear is fully made from steel and performed well in several drop-test campaigns. The engineering landing gear was meant as an economical test version. In case of the SAGITTA Demonstrator it is used to test the general assembly of NLG and MLG and to use it as test platform for the industrial dampers with different characteristic. For weight saving reasons the landing gear intended for flight test was rebuild from aluminum after the engineering tests were done. To take the lesser Young's modulus of aluminum into account some adjustments, such as larger torque and side struts were done. With this flight hardware of the landing gear some final drop-tests were performed to prove its correct function. The measurements showed that the engineering landing gear performed much better than the first version of the flight landing gear in terms of landing loads reduction and deflection behavior (TAB. 3). Whereas the engineering landing gear used the whole stroke, the first flight versions of the landing gear used only a small part of the stroke, stiffened and tended to bounce.

$V_{vertical}$ [m/s] at $V_{horizontal}$ = 49.0 m/s	Force at Engineering MLG [N]	Force at 1 <sup>st</sup> version Flight MLG [N]	Force at final version Flight MLG [N]
1.5	4000	7600	2500
2.5	5800	11600	4500

TAB. 3 Drop-test performance of the different landing gear versions

The first attempt to solve this problem was a hard anodization of the lower and upper tubes. It is done to gain a slightly harder and smooth/plainer surface. The results of the drop-tests carried out with the anodized landing gear, showed small improvements but did not reach the performance of the engineering landing gear. Analyzing the high speed videos of the drop-tests showed that the landing gear is deflected to the side and to the back because of the wheel spin-up loads. It was assumed that the softer aluminum with a Young's modulus of around 70 GPa compared to steel with a Young's modulus of around 210 GPa is ovalized by that deflection. A simulation done by Airbus Defense and Space proved the theory [10]. The ovalization of the lower tube inside the upper tubes led to a deadlock between those two and resulted in high drop down forces, since the shock absorber was not able to dissipate the kinetic energy. It was attempted to make only the hardly stressed lower tubes from steel and re-use the anodized upper tubes. The goal was to reduce the ovalization of the lower tube and to save as much weight as possible compared to the engineering landing gear. Additionally silicone lubrication between upper and lower tubes was used. The drop-tests and the high speed video analysis with the adapted final flight version of the landing gear showed even better results than the engineering landing gear. The saved weight amounts to 1.1 kg per landing gear leg. The calculated damper characteristic and its results of the landing gear testbed were used by Airbus Defense and Space in their six degrees of freedom model of the SAGITTA Demonstrator to conduct simulations of landings with different sideslip and bank angles.

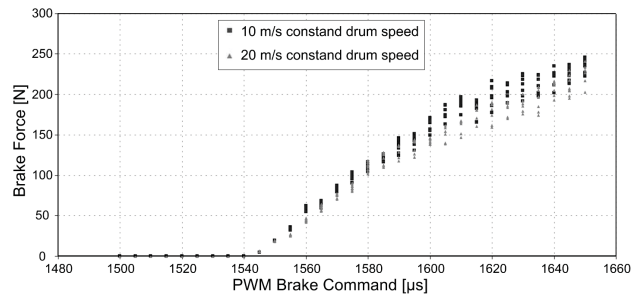


FIGURE 12. Brake force distribution at different drum speeds

The brake system was also tested on the rotating drum. The goal was to determine the brake force at the wheel under test conditions and support the calculation shown in section 3.2. For the brake test the drum with the landing gear on top was accelerated to a certain speed. With a brake command equal to a certain brake force a braking with 2 seconds duration was performed. The brake force at the tire was calculated from the additional torque output of the electric motor that is needed to maintain the drum speed. The tests were carried out at different drum speeds and with different brake force commands to the actuator. FIGURE 12 shows the acquired brake force over the PWM brake command. Compared are the values at 10 m/s and at 20 m/s drum speed. It can be seen that the brake force values differ for the same brake command. The variation in the total brake force for the same brake command was up to 16% of the maximum achieved brake force at that command. Further research has to be done to fully characterize the brake system behavior. However the landing gear testbed is not suited for a more accurate analysis of the brake system. The results might be influenced by the landing gear behavior or the pairing of tire and drum. In perspective a special brake testbed has to be designed to research the disk brake system. The chosen tires suffered no critical damage during the drop-tests, the brake tests and rolling tests. The tires are regarded as verified under the design requirements of the SAGITTA Demonstrator.

## 5. CONCLUSION AND OUTLOOK

This paper showed the principles of landing gear design and layout with the use of handbook formulae. Equation (1) by Currey and the recommendations for some of the values are originally meant for preliminary landing gear design of common civil and military aircrafts. SAGITTA Demonstrator and its landing gear size on the contrary are more in line with model aircraft. However, the initial requirements mentioned in section 2 exceed the requirements of common model aircraft by far. The formula for the damper characteristics  $c$  (5) and the formula of the brake disk thickness (14) for example are derived from basic physical correlations. However, the conducted landing gear qualification tests not only showed that these handbook formulae offer quite satisfying results, moreover there seem to be no scaling effects that have to be taken into account. Therefore the usage of handbook formulae seems to be an appropriate alternative to simulation models in early design phase.

Despite being suited to fulfill the requirements, the tests of the brake system showed that a characterization of a disk brake system is quite comprehensive. Future research will address this problem by the use of a special designed



testbed for the brake system only. Other future research work will probably test the landing gear system under real flight conditions beyond the maiden flight of the SAGITTA Demonstrator, depending on the further use of the demonstrator.

The maiden flight of the SAGITTA Demonstrator was accomplished 05.07.2017 at a test range near Overberg, South Africa. Take-off, the actual flight as well as the landing were done fully autonomous with a traditional remoted safety pilot as a backup. The flight along preset mission waypoints was performed in around 7 minutes and was completed with a smooth landing. Since the backup safety pilot was not forced to take over the control, the high estimated vertical landing speeds of 2.5 m/s did not occur. Instead the flight control computer managed to land the demonstrator at a moderate vertical speed of around 1.0 m/s. The landing gear seemed to have no issues to reduce the resultant forces of the touch down. Certainly the demonstrator was not equipped with sensors to backup this estimation with actual data. A second flight two days later was accomplished without any issues from the landing gear, too. Depending on the further use of the demonstrator, it would be useful if the landing gear will be equipped with sensors in order to be able to collect test data under real operating conditions.

## References

- [1] J. Seifert, "SAGITTA - Nationale Forschungsk Kooperationen für fortschrittliche UAV-Technologien im Rahmen der Open Innovation Initiative von CASSIDIAN", Deutscher Luft- und Raumfahrtkongress, Berlin, 2012.
- [2] J. Seifert and J. Dormwald, "Sagitta Overview - Internal Document", Airbus Defense and Space.
- [3] A. Bierig, F. Nikodem, P. Gallun and C. Greiner-Perth, "Design of the General Systems for the SAGITTA Demonstrator UAV", International Conference on Unmanned Aircraft Systems, Miami, 2017.
- [4] INCOSE, "Systems Engineering Handbook - A Guide for System Life Cycle Processes and Activities", John Wiley & Sons, Inc, Hoboken, New Jersey, 2015.
- [5] N. S. Currey, "Aircraft Landing Gear Design: Principles and Practices", Second ed., Washington D.C.: American Institute of Aeronautics and Astronautics, Inc., 1988.
- [6] European Aviation Safety Agency, "Certification Specifications for Normal, Utility, Aerobatic, and Commuter Category Aeroplanes CS-23", 2012.
- [7] J. Roskam, "Airplane Desing Part IV: Layout of Landing Gear and Systems", Sixth ed., Lawrence, Kansas: Design, Analysis and Research Corporation (DARcorporation), 2010.
- [8] Zimmer Group, "Catalouge // Damping Technology 1 // Industrial and Soft Close", 2015.
- [9] Volz Servos, "DA 26 Technical Specification", 2015.
- [10] Airbus Defense and Space, "Sagitta - Structural Analysis of Main Landing components (Internal Document)", 2016.